

HLWYM HEmails

From: John Trapp [JST@nrc.gov]
Sent: Monday, November 19, 2007 9:27 AM
To: Gordon Wittmeyer; pdubreuilh@cnwra.swri.edu; Deborah DeMarco; Jack Guttman; Sunny Kim; Tanya Parwani-Jaimes; nancy.adams@swri.org
Subject: AI 14002.01.151.801 (CNWRA Ticket 2008-0012)
Attachments: Menand_07_Ch25_draft_ML0731104910.pdf

We have reviewed the above referenced document and believe that there are a significant number of programmatic word changes that need to be addressed, which reflect on the conditional nature of magma-drift event with a potential Yucca Mountain Repository. There also are a couple of technical clarifications needed, including density of HLW as 10 g/cc (not 20 g/cc for DU) and the entrainment model assuming a Couette (laminar) flow regime with no eddy problems etc. Results are acceptable, but there needs to be an acknowledgment that the surface for potential entrainment will be very rough as there would be a lot of material on the floor.

We have attached a PDF mark-up of the suggested changes. When these are addressed please resubmit this document.

Because of the requested changes, this ticket will not be closed, but extended until after receipt of the resubmitted by the CNWRA.

If there are any questions please contact me at 310-492-3148 or by e-mail at jst@nrc.gov.

Hearing Identifier: HLW_YuccaMountain_Hold_EX
Email Number: 1009

Mail Envelope Properties (s74156f4.019)

Subject: AI 14002.01.151.801 (CNWRA Ticket 2008-0012)
Sent Date: 11/19/2007 9:27:03 AM
Received Date: 11/19/2007 9:27:47 AM
From: John Trapp

Created By: JST@nrc.gov

Recipients:

"Gordon Wittmeyer" <gwitt@cnwra.swri.edu>
Tracking Status: None
"pdubreuilh@cnwra.swri.edu" <pdubreuilh@cnwra.swri.edu>
Tracking Status: None
"Deborah DeMarco" <Deborah.DeMarco@nrc.gov>
Tracking Status: None
"Jack Guttman" <Jack.Guttman@nrc.gov>
Tracking Status: None
"Sunny Kim" <Sunny.Kim@nrc.gov>
Tracking Status: None
"Tanya Parwani-Jaimes" <Tanya.Parwani-Jaimes@nrc.gov>
Tracking Status: None
"nancy.adams@swri.org" <nancy.adams@swri.org>
Tracking Status: None

Post Office: NRNWMS05.NRC.GOV

Files	Size	Date & Time
MESSAGE	993	11/19/2007 9:27:47 AM
Menand_07_Ch25_draft_ML0731104910.pdf		363556

Options

Priority: Standard
Return Notification: No
Reply Requested: No
Sensitivity: Normal
Expiration Date:
Recipients Received:

Chapter 25: Modeling the Flow of Basaltic Magma Into Underground Openings

Thierry Menand, Jeremy Phillips, Steve Sparks, Andy Woods

25.1 Introduction

Worldwide, a consensus is developing among countries using nuclear power that deep, geologic disposal of spent nuclear fuel and high-level radioactive waste is the safest long-term option (National Research Council, 1990, 2001; EPA, 2004). The geologic medium acts as a component of a multiple barrier system (including the waste form and engineering components) designed to isolate the waste from the biosphere. Regulations in many countries, therefore, require repository developers to consider various natural hazards when evaluating repository performance. Among the hazards considered is the potential for igneous activity at the site and surrounding area (Long and Ewing, 2004). For example, in the United States, regulations governing the geologic disposal of high-level radioactive waste at the potential Yucca Mountain, Nevada, repository require inclusion of risk (i.e., probability and consequence) in assessments of the safety of the repository system. Based on probabilities estimated for repository disruption by future basaltic volcanism [e.g., 1.8×10^{-8} (Bechtel SAIC Company, LLC, 2007), 1.0×10^{-6} (Smith and Keenan, 2005)] and the risk assigned to this natural hazard, performance assessments must evaluate the consequences of a basaltic volcano intersecting the drifts and tunnels of the potential repository, damaging the emplaced waste packages and waste form, and transporting radioactive material to the biosphere (NRC, 2005).

There is almost no precedent for a volcanic eruption interacting with an underground disposal of the kind envisaged for radioactive waste repositories. A basaltic eruption along a 10-cm-diameter borehole in the 1977 eruption of Krafla volcano, Iceland [Larsen *et al.*, 1979], is the closest analogue. These facilities generally consist of a network of tunnels or drifts. Some designs require the drifts to remain empty apart from their inventory of radioactive waste containers, at

least up to the time the repository is permanently closed (i.e., on the order of several hundred years in some cases). Thus, the generic processes that might occur when magma erupts into empty drifts have been a prominent topic of study. Because no such events have occurred and analogues such as eruptions into natural caves have not yet been identified, the assessment of igneous disruption will need to rely largely on non-empirical information. In general, such assessments may consider the limited empirical evidence of volcanic and intrusive processes; knowledge of the properties of erupting magmas that help constrain the dynamics of these processes; laboratory experiments designed to elucidate how multiphase fluids interact with drifts; and finally, development of models. Because of the complexity of the processes and current state-of-the-art in representing those processes, a comprehensive approach to assessing igneous consequences that integrates knowledge from each of these sources is appropriate.

This chapter focuses on modeling with an emphasis on the use of analogue laboratory experiments that are designed either to (i) test theories and numerical models or (ii) gain insights into processes in circumstances where numerical models are either poorly understood or too complex. To develop appropriate models, we considered results from volcanological studies of eruption behavior and products. We also incorporated the physical properties of magma when we chose relevant analogue fluids and addressed scaling issues.

25.2 Magma Properties and Fluid Dynamics Relevant to Magma-Drift Interaction

25.2.1 Physical Properties of Magmas

The magma properties that exert the strongest control on flow dynamics are the magma density ρ and viscosity μ , both of which decrease with increasing temperature. Typical basalt eruption temperatures range from 1000 to 1300 °C [Kilburn, 2000; Francis and Oppenheimer, 2004], and over this range of temperatures, the density and viscosity of natural, dry basaltic melts range

between 2800 and 2600 kg/m³ and between 1000 and 1 Pa s at atmospheric pressure, respectively [Murase and McBirney, 1973; Kilburn, 2000; Spera, 2000; Francis and Oppenheimer, 2004].

Magma typically consists of three phases: melt (liquid), crystals (solid), and bubbles (gas). The temperature dependence of the melt viscosity can be described by several models; the simplest is the Arrhenian model $\mu = \mu_0 \exp(E^*/RT)$, where μ_0 is the melt viscosity at infinite temperature, E^* is the melt activation energy, R is the universal gas constant, and T is the temperature in Kelvins. According to this model, melt composition mainly affects the activation energy E^* , and Shaw [1972] estimated the activation energy from the partial molar coefficients of SiO₂. Although melts with high silica content do not exactly follow the Arrhenian temperature-viscosity relationship [Hess and Dingwell, 1996], it is usually necessary to employ the simpler Arrhenian model of Shaw [1972] for petrologic purposes [Spera, 2000], which is a good approximation for low viscosity basalts [Giordano and Dingwell, 2003].

Small amounts of dissolved volatiles can have important effects on the density, viscosity, and crystallization of melts and magmas, which will strongly influence the ability of magmas to flow. Of all the volatile species, water is the most abundant and accounts for the largest variations in density and, more importantly, viscosity. Basaltic magmas typically contain 1–4 wt% volatiles, although dissolved water contents as high as 6 wt% have been measured in arc basalts [Sisson and Layne, 1993], and water contents up to 4.6 wt% have been estimated for the Lathrop Wells basalts near the proposed site for the high-level radioactive waste repository at Yucca Mountain, Nevada [Nicholis and Rutherford, 2004; Valentine *et al.*, 2007]. Dissolved water contents of 3 wt% will lower the density of basaltic melts by 5 wt% [Lange, 1994; Wallace and Anderson, 2000] and lower the melt viscosity of basalts by two orders of magnitude [Shaw, 1972; Giordano and Dingwell, 2003]. Water is not the only volatile species, however. CO₂ is also present in magmas, but the amounts of dissolved CO₂ are typically one to two orders of magnitude less than

those of water. Furthermore, the effect of CO₂ on melt density and viscosity is smaller than for water: Wallace and Anderson [2000] report that adding 3 wt% of CO₂ to a basaltic melt will decrease its density by ~3%. Contrary to water, dissolved CO₂ appears to have a minimal effect on melt viscosity. This effect depends on the speciation of CO₂, and dissolved CO₂ can increase melt viscosity slightly if the CO₂ is dissolved as carbonate [Lange, 1994]. Dissolved CO₂ in melts can also have important indirect effects on melt viscosity because dissolved CO₂ lowers the solubility of water [Holloway and Blank, 1994].

The presence of exsolved gas bubbles and crystals also has a strong influence on magma density and viscosity. Crystals act to increase both magma viscosity and density. Estimating the speciation and volume fraction of different crystal phases present in the melt requires modeling the thermal and decompression history of the magma. This is a complex process using an incomplete understanding of the phase behavior, particularly the solubility of CO₂ in basalts, so a more typical approach in recent studies has been to investigate a wide range of magma viscosities that will account for the ranges of temperatures, compositions, and crystal contents that characterize basaltic magmas.

The presence of exsolved gas bubbles significantly affects the density of magmas, which decreases linearly with the volumetric concentration c of the bubbles: $\rho \sim \rho_l(1-c)$, where ρ_l is the density of pure melt. The effect of bubbles on magma viscosity is more complex as it depends on the tendency of bubbles to deform under viscous stresses induced by flow, relative to their tendency to remain spherical as a result of interfacial stresses, and the rapidity of this response [Llewellyn and Manga, 2005]. For steady flows involving spherical bubbles, the commonly accepted empirical relationship at low volumetric fractions (< 10%) for viscosity of the bubbly mixture, μ_b , as a function of bubble content and melt viscosity, μ_l , is $\mu_b = \mu_l/(1-c)$ [Llewellyn and Manga, 2005; Menand and Phillips, 2007b]. For higher bubble contents, viscosity appears to be

better approximated by the relationship $\mu_b = \mu_l (1 - c)^{-5/2}$ [Jaupart and Vergnolle, 1989; Menand and Phillips, 2007b].

An important consideration in the eruption of water-rich basalts is the crystallization that is principally related to the change in liquidus temperatures of the main stable mineral phases. Degassing-induced crystallization and the consequent rheological changes are key to understanding conduit flows and lava extrusions in andesite eruptions [Cashman, 1992; Melnik and Sparks, 1999]. This is likely to be the case for wet basalt eruptions, too, although there is less supporting research. The viscosity increases dramatically as groundmass crystals form from degassing basalt, and the crystal content may become so high that the rheology can become non-Newtonian. For example, wet trachybasalt with a liquidus at 950–1,000 °C [Nicholis and Rutherford, 2004] tends toward the solidus at one atmosphere pressure. The effects of degassing on crystallization and viscosity will be counteracted by the latent heat of crystallization [Blundy *et al.*, 2006] such that the temperature will be above the solidus in the fully degassed and decompressed state at one atmosphere. Fifty percent crystallization will increase the temperature by approximately 100 °C based on the latent heat of crystallization of plagioclase as the dominant groundmass mineral. Thus, the eruption temperature of trachybasalt should be around 1,050–1,100 °C. The rheology of such magmas can be compared to the field rheological measurements of Etna trachybasalt lava [Pinkerton and Sparks, 1978], which is about 10^5 Pa s with approximately 50% total crystal content at 1,070 °C.

At lower pressures, gases become less soluble in magmas, leading to an increase in gas exsolution and magma crystallinity. Additionally, gas bubbles expand as the magmatic pressure decreases, so the controls exerted by bubbles and crystals on magma properties become more significant at lower pressures, and these effects will be especially important at the typically

shallow depths (~500 m) of nuclear waste repositories. The exsolved gas mass fraction n varies with pressure according to the solubility law (based on Henry's Law)

$$n(P) = n_0 - sP^{1/2}, \quad (25.1)$$

where n_0 is the total gas mass fraction, P is pressure, and s is the solubility constant for water in basalt, with a value $3 \times 10^{-6} \text{ Pa}^{1/2}$ [Holloway and Blank, 1994]. In general, the gas pressure will not be equal to the bulk flow pressure or to the surrounding rock lithostatic pressure. Exsolving gas bubbles are overpressured with respect to the surrounding fluid due to surface tension, viscous resistance, and inertia, as gas bubbles expand in ascending magma due to diffusion and decompression [Sparks, 1978; Sparks *et al.*, 1994]. In basalt magmas, overpressures due to surface tension and inertia are typically negligible but overpressures due to viscous resistance can be significant in very fast explosive flows. Additionally, the bulk flow pressure is initially determined by the pressure in the source chamber but decreases due to frictional losses in the magma flow. Thus, gas pressure evolves during magma ascent, which in turn determines volatile exsolution and depends on the detailed dynamics of the eruption [Massol *et al.*, 2001]. A common approach is to assume that pressure is lithostatic, but magma pressures that deviate significantly from lithostatic are likely. For example, a dike typically requires internal pressure that exceeds lithostatic pressure and the tensile strength of the surrounding rock to propagate [Lister and Kerr, 1991], whereas an explosive eruption through an open conduit can result in large underpressures [e.g., Mason *et al.*, 2006]. Significant disequilibrium is also possible for fast flows so that kinetics have to be taken into account. If flows are at equilibrium, however, the solubility law given by equation (25.1) can be used for any pressure assumption.

25.2.2 Magma Flow Dynamics

Magma ascends through the Earth's crust by means of dikes, which are sheetlike igneous intrusions typically several centimeters to meters or tens of meters (rarely several hundred of meters) in thickness and several kilometers (rarely several hundred of meters) in extent [Pollard, 1987]. The present study considers a 1-m width and a 1- to 10-km lateral extension as reasonable average dimensions for basaltic dikes [Lister and Kerr, 1991; Rubin, 1995]. Magma fluxes can range from $1 \text{ m}^3 \text{ s}^{-1}$, an average replenishment rate for the summit reservoir at Kilauea volcano, Hawaii [Rubin and Pollard, 1987], to $10^6 \text{ m}^3 \text{ s}^{-1}$, such as may be appropriate to very high volumetric flow flood basalt eruptions [Swanson *et al.*, 1975; Wilson and Head, 1981]. An average magma flux of $10^3 \text{ m}^3 \text{ s}^{-1}$ would correspond to an average magma ascent rate of 1 m s^{-1} through a 1-m-wide and 1-km-long dike.

Magma ascent through dikes is mainly driven by magma buoyancy, initially determined by magma composition and ultimately controlled by volatile exsolution, which becomes the dominant control at shallower depths. A key fluid dynamical parameter for magma flow is the Reynolds number $Re = \rho uL/\mu$, which represents the ratio of inertial to viscous forces (u is the flow velocity and L is a typical length scale such as dike thickness). Magma flow is laminar if $Re \ll 10$, and the flow is considered to become turbulent when the Reynolds number exceeds a critical value on the order of 1,000 [Lister and Kerr, 1991]. In most cases, magma flow is laminar with a Reynolds number on the order of one for basaltic magma with viscosity of $1,000 \text{ Pa s}$ and density of $2,750 \text{ kg m}^{-3}$ flowing at a rise velocity of 1 m s^{-1} in a 1-m-wide dike. However, flows that involve magmas of much lower viscosity or higher magma ascent rates, such as during flood basalt eruptions, may become turbulent [Huppert and Sparks, 1985].

An important question is whether exsolved volatile bubbles are uniformly distributed throughout the magma, forming a uniform bubbly mixture, or whether phase separation occurs,

which would strongly modify the flow behavior. Two-phase flow regimes range, in order of increasing bubble content and flow explosivity, from bubbly flows to slug flows, where bubbles coalesce into larger gas pockets, to annular flows, where gas flows in the center of a dike or conduit while the fluid phase flows on its periphery, to dispersed flows, where fragmented magma is carried by gas flow [Wallis, 1969; Jaupart, 2000; Slezin, 2003; see Figure 25.1]. Although magma flow will evolve through these different regimes as the bubble content increases, how magma flows change from one regime to another is still not fully understood. The different two-phase flow regimes depend on various parameters that include, but are not restricted to, bubble contents, flow rates, and flow geometries [Wallis, 1969]. A reasonable assumption is to consider that deeper in a basaltic system, bubbles are well mixed due to low volumetric concentration, the relatively small size of the bubbles, the relatively low viscosity of basaltic melts, and the effects of magma convection [Phillips and Woods, 2001]. As we shall show, the geometry of the magmatic system provides a strong control on bubble segregation from the melt, so an appropriate starting condition is to assume exsolved gas bubbles uniformly distributed throughout the melt.

25.3 Modeling Magma-Repository Interaction

25.3.1 Transient Flows

The initial interaction with repository drifts involves the transient case where a magma-filled dike propagates and intersects a drift; however, it is unknown whether this magma will be degassed. Degassed lava emerges early in some basaltic eruptions and can be associated with simultaneous explosive activity. As mentioned previously, gas segregation processes are not understood well enough to determine whether the magma that first flows into a drift will be degassed. Thus, both end member cases should be considered to bound possible interactions. Lejeune *et al.* (this

volume) consider the degassed case through laboratory experiments and theoretical analysis. Here we consider the explosive end member where the magma and gas have not segregated.

An explosive flow is expected for the interaction of rapidly decompressing gas-rich magma rising in a dike with an underground drift structure. Repository drifts are usually proposed to be maintained at atmospheric pressure [Rosseau *et al.*, 1999], while at the proposed repository depths of 200–300 m, the magma pressure just behind the tip of a dike is estimated to be typically 10–20 MPa, based on the lithostatic pressure and the fluid pressure required to drive a fracture at the dike tip [Pollard, 1987; Lister and Kerr, 1991; Woods *et al.*, 2002]. When the dike intersects the drift, the magma will rapidly decompress, and at the relatively high water contents measured for Lathrop Wells basalts of up to 4.6 wt% [Nicholis and Rutherford, 2004], this decompression will be explosive [Blackburn *et al.*, 1976], assuming that the gas has been retained during ascent.

A quantitative model of the process of magma decompression into a subsurface horizontal drift was proposed by Woods *et al.* [2002]. On decompression, volatile exsolution within the magma in the dike and the drift will cause it to expand and accelerate, and if this process occurs sufficiently rapidly, the magma will fragment into a two-phase mixture of vesicular magma and gas. Woods *et al.* [2002] modeled this flow as a one-dimensional homogeneous mixture of magma and gas in a coordinate frame that was continuous for the flow from the dike into the drift (Figure 25.2). The cross-sectional area was assumed to vary smoothly between the dike and drift, and the flow was assumed to remain isothermal during volatile exsolution due to the high thermal inertia of the magma.

The motion of the magma-gas mixture can be described in terms of its averaged velocity, u , and averaged density, ρ , at position x , pressure P , and time, t , leading to the equation for the conservation of momentum

$$\rho \left(\frac{\partial u}{\partial t} + u \frac{\partial u}{\partial x} \right) = -\frac{\partial P}{\partial x} - fu - \rho g G(x), \quad (25.2)$$

where f is a drag coefficient and $G(x)$ has value 1 in the vertical dike and 0 in the horizontal drift. The terms on the left-hand side describe the inertia of the magma-gas mixture, and the terms on the right-hand side represent the pressure gradient in the flow, the resistance to motion due to flow against the walls of the dike or drift, and the buoyancy forces, respectively. The drag coefficient was parameterized as

$$f = \frac{\alpha \mu}{D^2} + \frac{2C\rho|u|}{D}, \quad (25.3)$$

where α is a coefficient with value 12 for a two-dimensional dike and 8 for a cylindrical drift, D is dike width or drift diameter, and C is the turbulent drag coefficient. The first term on the right-hand side is the viscous drag, and the second term is the turbulent drag.

The equation of conservation of momentum was coupled with an equation for mass conservation

$$\frac{\partial(A(x)\rho)}{\partial t} + \frac{\partial(A(x)\rho u)}{\partial x} = 0, \quad (25.4)$$

where $A(x)$ is the cross-sectional area of the dike or drift, and an equation for the bulk density of the magma-gas mixture (based on the Perfect Gas Law)

$$\frac{1}{\rho} = \frac{n(P)RT}{P} + \frac{(1-n(P))}{\rho_l}, \quad (25.5)$$

where $R = 462 \text{ J kg}^{-1} \text{ K}^{-1}$ is the gas constant for H_2O , T is the (constant) temperature, and $n(P)$ is the exsolved gas mass fraction given by the solubility law (25.1).

For their model simulations, Woods *et al.* [2002] assumed basaltic values $\mu = 10 \text{ Pa s}$, $\rho = 2,600 \text{ kg/m}^3$, a water content of 2 wt%, and $C = 0.01$. The results of a typical simulation for a dike intersecting a drift and remaining open are shown in Figure 1 in Woods *et al.* [2002].

Initially, the magma-gas mixture rapidly expands as a rarefaction wave propagates back into the dike through the magma, and volatiles are exsolved. The expanding mixture accelerates along the drift, reaching speeds of tens to hundreds of meters per second, with the density decreasing as the pressure falls. Air is displaced and compressed ahead of the magma-gas mixture, and as a result, a shock forms in the air and moves down the drift at speeds of several hundreds of meters per second. If the drift is closed at its ends, then the shock is reflected when it reaches the end of the drift, increasing its amplitude by an order of magnitude. The reflected shock recompresses the magma-gas mixture, and a region of higher pressure, up to a few MPa, is formed in the drift. If the drift is open ended, the flow adjusts to a steady regime within seconds once the drift system is completely filled [Woods *et al.*, 2002].

Darteville and Valentine [2005] further investigated the eruption scenario proposed by Woods *et al.* [2002] using the GMFIX multiphase numerical model [Darteville, 2004]. This model allowed the properties of each phase (pyroclasts and gas) to be determined in a two-dimensional Cartesian frame with full time-dependence, relaxing the assumption of homogeneous flow made by Woods *et al.* [2002]. The results of a simulation corresponding to the intersection of an overpressurized dike containing basalt with 1 wt% water with a drift at atmospheric pressure are shown in their Figure 1 [Darteville and Valentine, 2005]. About 30–35% of the magma-gas mixture flows into the drift, forming a shock that propagates into the drift at speeds of about 200 m s^{-1} . The following flow forms a low density current that flows along the drift roof at

speeds of about 120 m s^{-1} . If the end of the drift is closed, the shock is reflected and weakens through interaction with the following gas flow before interacting with the current of pyroclasts and ash at a time of 1.10 s. On reaching the closed end of the drift, the current is concentrated in density and reflected to form a dense current that flows along the base of the drift. When the dense return flow reaches the dike, some of the material is entrained into the rising flow and reaches the surface, while some is recirculated back into the drift.

Both Woods *et al.* [2002] and Darteville and Valentine [2005] investigated scenarios where there are secondary openings in the drift due to the presence of a further dike and found that there is little difference to the flow patterns and velocities and pressures generated. Both studies show the generation of high-speed shocks due to the initial decompression of the magma-gas mixture into the drift, although the shock amplification on reflection from the closed end of the drift observed by Woods *et al.* [2002] is not recognized in the simulations of Darteville and Valentine [2005]. The formation of high pressure regions in the magma-gas flow has important implications for the disruption of waste containers and transport of pelletal material, as discussed further in Section 25.3.3.

We are aware that other models have been presented in various reports on igneous consequences at Yucca Mountain by different panels and bodies. We have not referred to this work, which has not been subject to peer review. However, the results of such studies all confirm that fast explosive flows will occur when volatile-rich basaltic magma meets a repository.

The only reported natural example of the interaction of basalt with an analogous man-made structure occurred as an eruption along a geothermal borehole during the 1977 Krafla eruption [Larsen *et al.*, 1979]. The borehole was 10 cm in diameter and 1138 m in length. The eruption involved an explosive Strombolian jet, lasted 20 minutes, and erupted a volume of 26 m^3 . In the context of potential repository interactions, this example is important because it

shows that basalt magma can flow along a hole that has a cross-sectional area two orders of magnitude smaller than a radioactive waste repository drift. This case shows that cooling to form a quenched layer is not significant, so models that do not account for cooling reasonably simulate the pertinent processes.

25.3.2 Steady-State Flows

Following the initial transient decompression of the gas-bearing magma into the drift, the flow will adjust to a steady state within seconds to hours depending on whether magma flow is diverted along the drift or is limited to the main dike if access drifts are backfilled with crushed rocks [Woods *et al.*, 2002; Darteville and Valentine, 2005]. If steady-state magma flow is established in the drift, Woods *et al.* [2002] calculated that magma will flow past the waste containers with steady speeds of order 10 m s^{-1} . Waste containers will experience considerable thermal stress from the magma and gradually heat by thermal conduction and, for times greater than $\sim 1,000 \text{ s}$ (based on diffusion of heat into the waste containers), they will become deformable and may break open. If the end of the drift remains closed, magma flow will be limited to the main dike but basaltic magma will nevertheless fill the drift. In both cases, magma pressure in the repository will ultimately decrease to be close to lithostatic [Woods *et al.*, 2002].

This latter result is consistent with observations of natural volcanic systems. It is commonly observed that many basaltic eruptions tend to become less explosive with time. Initial basaltic eruptions occur explosively along fissures, typically in Strombolian-style fire fountains. Within hours to a few days, activity focuses onto a progressively restricted number of vents along the fissures [Thorarinsson, 1969; Fedotov and Markhinin, 1983; Macdonald *et al.*, 1983]. There is a general tendency for such eruptions to become less explosive with time and for lava to become an increasingly dominant product. However, observations of eruptions such as Eldfell Volcano (Iceland) in 1973 show that even at the very beginning of an eruption, explosive flow of gas-rich

magma and discharge of degassed lava occur simultaneously. The interaction of a dike with an underground drift is therefore likely to involve magma flow of decreasing intensity. Basaltic magma can fill the drift, and subsequent magma circulation will depend on processes of gas segregation within the drift [Menand and Phillips, 2007a]. Moreover, as the eruption proceeds, magma flow can be sustained for days to weeks in the vertical dike; for example, the great Tolbachik basaltic fissure eruption of 1975–1976 lasted for more than one and a half years [Fedotov and Markhinin, 1983]. Over these time frames, the dike may increase in size and change from a planar cross-section to a more circular cross-section owing to mechanical and thermal erosion as well as solidification of the dike in areas away from the focused flow [Macdonald *et al.*, 1983; Bruce and Huppert, 1990].

At shallow crustal depths (less than 500 m) typical for repository drifts, magma volatiles are very likely to exist as exsolved bubbles. For instance, initial water contents of basalts that have erupted in the vicinity of Yucca Mountain range from 1.9 wt% to 4.6 wt% [Nicholis and Rutherford, 2004], and at a depth of 300 m, a basaltic magma with 4.6 wt% initial water will have exsolved 3.8 wt% [Holloway and Blank, 1994], which would correspond to volumetric gas fractions in the range of 70 to 90% at that depth in equilibrium [Menand *et al.*, 2006]. The presence of exsolved bubbles as well as the amount of water that remains dissolved will strongly affect the density and viscosity of the basalts. Furthermore, there may be a range of bubble volumetric contents depending on exsolution at greater depths and gas loss during ascent. The amount of exsolved gas in magma within the drift will determine the nature and strength of magma circulation in the drift.

Menand and Phillips [2007a; 2007b] investigated gas segregation in a magma-filled drift intersected by a vertical dike using analogue experiments. The apparatus consisted of a glass recirculating flow loop with a vertical mounting section (to simulate the vertical dike) connected

to a horizontal section (to simulate the drift; see Figure 1 in Menand and Phillips [2007a]). Electrolysis of the recirculating flow was used to simulate low volumetric gas fractions (<10%), producing micrometric bubbles in viscous mixtures of water and golden syrup. These low gas fractions correspond to the situation where magma has lost a large proportion of its gases at some depth greater than that of the repository or during the latest waning stages of an eruption. To simulate higher volumetric gas contents, golden syrup was aerated before its injection into the recirculating flow loop, leading to volumetric gas fractions as high as 40%.

The experiments of Menand and Phillips [2007a] at low gas fractions (<10%) show that exsolved bubbles induce a buoyancy-driven exchange flow between the dike and the drift, whereby bubbly fluid flows from the dike into the drift as a viscous gravity current (Figure 25.3 and Figure 3 in Menand and Phillips [2007a]). This exchange flow is slow enough that bubbles in the drift have time to rise, segregate from the fluid, and accumulate as foam at the top of the drift in conjunction with the accumulation of degassed fluid at the base of the drift. The maximum distance L_{\max} that the gravity current can travel corresponds to the point where all bubbles have risen to the top of the side arm

$$L_{\max} = \frac{D^2}{d} \left(\frac{12c}{1-c} \right)^{\frac{1}{2}} F(c), \quad (25.6)$$

where D is the drift diameter, d is the average bubble diameter, c is the volumetric bubble concentration, and F is a function of c , which has value of order 0.1 [Menand *et al.*, 2006]. Ultimately, a steady state is reached, whereby influx of bubbly fluid into the drift is balanced by outward flux of lighter foam and denser degassed fluid back into the dike. Moreover, gas

segregation processes and rates appear to be independent of moderate changes in magma supply rates in the dike.

The laboratory experiments at high gas fractions showed that the same processes occurred as for lower volumetric gas fractions, with the increased viscosity and reduced density contrast increasing the time scale for gas segregation [Menand and Phillips, 2007b; Menand *et al.*, 2006]. The amount of foam that collects at the top of the drift is determined by the balance between the amount of bubbles rising from the bubbly fluid within the drift and the outward flux of foam that leaves it, and the steady-state foam thickness $h(x)$ can be written as the product of a characteristic thickness H and a shape function $f(x)$, $h(x) = Hf(x)$, with

$$H = \left[\frac{c(1-c)^{\frac{7}{2}} d^2 L_{\max}^2}{\varepsilon(1-\varepsilon)^{\frac{5}{2}} (\varepsilon - c)} \right]^{\frac{1}{4}}, \quad (25.7)$$

$$f(x) = \left(\frac{x}{L_{\max}} - \frac{x^2}{4L_{\max}^2} \right)^{\frac{1}{4}}.$$

where ε is the volumetric gas fraction of the foam and x is the position along the foam (the origin is fixed at the dike-drift junction). The foam thickness is limited by the packing of the bubbles in the foam: as the foam thickness increases, bubbles deform and can coalesce, leading to the collapse of the foam. The maximum critical thickness H_c the foam can sustain before collapsing is [Jaupart and Vergnolle, 1989; Menand *et al.*, 2006]

$$H_c = \frac{4\sigma}{\varepsilon\rho_l g d}, \quad (25.8)$$

where σ is the surface tension between the melt and the gas trapped in the bubbles of the foam.

The steady-state foam thickness H described by equation (25.7) can develop only if it is smaller

than the critical thickness H_c . If this is not the case, accumulation of bubbles at the top of the drift will lead to repeated collapse of the foam.

Two time scales are associated with this gas segregation process, and both are controlled by the rise of bubbles within the drift. The first one is the time needed by the bubbles to rise the diameter of the drift D and accumulate as the foam

$$T_b = \frac{12\mu_l D}{\rho_l g d^2 (1-c)^{\frac{7}{2}}}. \quad (25.9)$$

The second time scale is the time needed for the steady-state foam to fully develop

$$T_f = \frac{12\mu_l L^{\frac{1}{2}}}{\rho_l g d^{\frac{3}{2}}} \left[\frac{\epsilon^3}{c^3 (1-c)^{\frac{21}{2}} (1-\epsilon)^{\frac{5}{2}} (\epsilon-c)} \right]^{\frac{1}{4}}. \quad (25.10)$$

Gas segregation occurs in the drift if these two time scales are smaller than the time scale for cooling and solidification of the magma T_s . Menand and Phillips [2007a; 2007b] based their calculations on cooling by pure conduction so that

$$T_s = \frac{D^2}{16\kappa\lambda^2}, \quad (25.11)$$

where κ is the magma thermal diffusivity and the thermal constant λ depends on the temperature difference between the magma and surrounding rocks [Turcotte and Schubert, 1982].

Gas segregation leads to a steady-state recirculation of fluid in the drift with exchange of bubbly fluid with foam and degassed fluid, and this recirculation is characterized by a volumetric flux

$$Q = \frac{(1-c)^{\frac{7}{2}} \rho_l g d^2 DL}{12\mu_l \varepsilon}. \quad (25.12)$$

Upscaled to repository conditions, the results suggest that steady-state gas segregation would occur within hours to hundreds of years depending on the viscosity of the degassed magma, $10\text{--}10^5$ Pa s, and the average size of exsolved gas bubbles, 0.1–1 mm, (right-hand plot of Figure 13 in Menand *et al.*, 2006). For comparison, Menand *et al.* [2006] give a solidification time scale by pure conduction of about 3 months for a 5-m-diameter drift; note that this estimate will be a lower bound due to circulation in the drift and replenishment with hotter magma as the eruption proceeds.

Using equation (25.12), Menand *et al.* [2006] calculated the fluxes that would be associated with gas segregation in a 5-m-diameter repository drift for different magma viscosities (right-hand plot of Figure 15 in Menand *et al.*, 2006). These range from $1 \text{ m}^3 \text{ s}^{-1}$ for the less viscous magmas to $10^{-8} \text{ m}^3 \text{ s}^{-1}$ for the most viscous degassed magmas. Gas segregation is likely to be in an unstable foam collapse regime, with the foam accumulated by gas segregation at the top of the drift reaching a few centimeters in thickness before its collapse due to bubble coalescence [Jaupart and Vergnolle, 1989; Menand *et al.*, 2006]. The relative proportion of erupted degassed magma, which could potentially transport nuclear waste material towards the surface, depends on the value of the dike magma supply rate relative to the value of the gas segregation flux, with violent eruption of gas-rich as well as degassed magmas at relatively high magma supply rates, and eruption of mainly degassed magma by milder episodic Strombolian explosions at relatively

lower supply rates [Menand and Phillips, 2007a]. Menand *et al.* [2006] calculated that, depending on the average size of exsolved gas bubbles, the critical magma supply rate delimiting these two eruptive regimes would range from 10^{-4} – $1 \text{ m}^3 \text{ s}^{-1}$ for magma viscosity $\sim 10 \text{ Pa s}$ to 10^{-8} – $10^{-4} \text{ m}^3 \text{ s}^{-1}$ for magma viscosity $\sim 10^5 \text{ Pa s}$.

Menand and Phillips [2007a] also applied these general principles to degassing and eruption processes at Stromboli volcano, Italy. The results and their implications are consistent with a variety of independent field data. Gas segregation at Stromboli likely occurs in a shallow reservoir of sill-like geometry at a 3.5-km depth with bubbles of exsolved gas 0.1–1 mm in diameter. Menand and Phillips [2007a] also calculated that the transition between Strombolian activity erupting gas-poor, highly porphyritic magmas and violent explosions that also erupt gas-rich, low porphyritic magmas would correspond to a critical magma supply rate on the order of 0.1 – $1 \text{ m}^3 \text{ s}^{-1}$.

If magma flows along the drift, either because the drift is open ended or because magma pressure in the repository is able to drive open a new fracture in the surrounding rocks, steady-state flow will be characterized by speeds on the order of 10 m s^{-1} [Woods *et al.*, 2002; Darteville and Valentine, 2005], which corresponds to steady-state fluxes of order $100 \text{ m}^3 \text{ s}^{-1}$ in a 5-m-diameter drift. These fluxes are at least two orders of magnitude greater than fluxes induced by gas segregation processes. In this scenario, gas segregation processes are unlikely to affect the flow as they would occur on time scales much longer than those needed for magma to flow along the drift. Therefore, the steady-state flow pattern would depend on the magma supply rate from the dike.

25.3.3 Magma Flow Dynamics and Cooling Within Repository Drifts

As magma flows up the dike and along the drift, heat will be advected by the flowing magma and will simultaneously be lost by conduction into the colder surrounding rocks and waste containers.

Competition between heat advection and conduction will affect magma dynamics, as investigated quantitatively by Bruce and Huppert [1989; 1990] and Petford *et al.* [1993]. During the initial stage of magma flow up a dike, magma cools and its temperature adjusts to that of the surrounding rock walls. Subsequently, the continual supply of magma transfers heat into the solid walls. Magma cooling within the dike is typically confined to a thin thermal boundary layer adjacent to the dike walls, and the width of this thermal boundary layer increases with the length of the dike [Carrigan, 2000]. Whether the dike becomes blocked or remains open is determined by the balance between the rate of solidification of the magma (dike closure) and that of melting of the walls (dike opening). These rates are in turn controlled by the magnitude of the latent heat (released during solidification and consumed during melting) as well as the difference between the heat supplied to the walls by the thermal boundary layer and that conducted into the surrounding rocks. Bruce and Huppert [1989; 1990] and Petford *et al.* [1993] showed that a

critical width $w_c = 1.5 \left[\frac{c_{heat} (T_w - T_\infty)^2}{L_{heat} (T_m - T_w)} \right]^{3/4} \left(\frac{\mu \kappa H_{dike}}{\Delta \rho g} \right)^{1/4}$ exists where c_{heat} is the specific heat,

L_{heat} is the latent heat, T_m is the initial magma temperature, T_w is the temperature of the walls, T_∞ is the far field temperature of the rocks, H_{dike} is the dike length, and $\Delta \rho$ is the density difference between magma and rocks. If the dike is thinner than this critical width, it will solidify before it can transport a significant volume of magma to the surface. When applied to basaltic dikes, these analyses show that dikes must be thicker than about 0.5 m if they are to reach the surface before solidifying completely; this prediction agrees with field observations [Wada, 1994; Kerr and Lister, 1995; Wada, 1995]. Three-dimensional analyses suggest that magma flowing through an initially long surface fissure will tend to localize to a number of isolated vents [Bruce and Huppert, 1989; 1990], as observed during basaltic fissure eruptions.

Insights about the cooling of magma as it flows within a drift can be obtained from studies of horizontal igneous intrusions (sills) and lava tubes. Holness and Humphreys [2003] observed that rocks surrounding the Traigh Bhàn na Sgùrra sill on the Isle of Mull, Scotland, displayed thermal aureoles up to 4 m thick around that sill, which taken in conjunction with the spatial distribution of crystals within the sill, demonstrate that progressive focusing of magma flow into the wider parts of the sill was sustained for up to 5 months. Lava tubes, which form when the lava flow surface solidifies as a crust while hot lava continues to flow beneath, are a common feature of basaltic lava flow fields. If the flow rate is sufficiently high, lava can thermally erode its way into the surrounding solidified lavas [Francis and Oppenheimer, 2004]. Lava tubes can extend significant distances because lava is well insulated by the tube crust and loses very little heat by conduction or radiation. Lava tubes up to 20 m in diameter and more than 100 km in length have been observed in Queensland, Australia; these would have enabled the lava flow fields to develop over several months to years despite involving overall effusion rates perhaps as low as $10 \text{ m}^3 \text{ s}^{-1}$ [Stephenson *et al.*, 1998]. The Krafla borehole eruption also shows that cooling may not be a major factor in the initial filling of a tunnel.

Precise assessment of magma cooling while flowing in a drift partially obstructed by waste containers is difficult because of the complex three-dimensional geometry of the flow field. Nevertheless, a conservative estimate can be made by assuming conductive cooling of the magma through the wall of the drift, which gives about 3 months for magma to solidify by conduction [Menand *et al.*, 2006]. This estimate is comparable to the time scales associated with lava flows within sills and lava tubes and suggests that magma could remain fluid for several months, at least in some part of the drift. For comparison, based on the diffusion of heat into the waste containers, Woods *et al.* [2002] calculated that the waste containers will become deformable and may break open for times greater than $\sim 1,000 \text{ s}$ (less than 1 hour). Improved estimates for magma cooling

within repository drifts and its effect on flow dynamics require three-dimensional numerical simulations.

If transient or steady magma flow occurs through radioactive waste repository drifts, possible consequences include the generation of waste container motion due to drag exerted by the flowing magma, heating and possible disruption of the waste containers, and transport of the container contents. Woods *et al.* [2002] estimate the drag force acting on the waste containers

$$F_d = C_d \rho u^2 A, \quad (25.13)$$

where A is the area of the face of the container perpendicular to the flow direction and C_d is the drag coefficient, which is order unity for these flow conditions. For steady flow conditions, Woods *et al.* [2002] estimated the ratio of the drag force to container weight to be typically of order or smaller than 0.1–1.0, suggesting that the containers may be displaced down the drift. However, the flow is too weak to keep the containers in suspension, and any container motion is likely to be relatively slow. Later calculations of the flow conditions following the intersection of a basaltic dike with a repository drift conducted by Darteville and Valentine [2005] were made with smaller dike widths and resulted in much lower flow velocities than those calculated by Woods *et al.* [2002]. In their calculations, the drag force was insufficient to generate waste container motion, and furthermore, because the waste containers will be placed in a line along the length of the repository drift, only the first container will feel the drag force estimated by Woods *et al.* [2002]. Subsequent containers will feel a lower drag force in the wake flow behind the first container—the same effect exploited by the formations adopted by migrating birds and racing cyclists.

To the extent that waste containers can be disrupted by the combined effects of magma flow and heat transfer, waste container contents can possibly be transported in the magma flow

through the drifts and to the surface. Although the exact contents of waste containers will vary, current design calculations typically assume that the waste material is spent nuclear fuel in the form of uranium dioxide pellets in the size range 10–500 microns [OCRWM, 2000] with a density of approximately $20,000 \text{ kg m}^{-3}$ [Bleise *et al.*, 2003] (borosilicate glass waste forms have not been studied). Erosive transport of small particles by turbulent stream flows has been widely studied in sedimentology, and the key parametric relationship between the Shields number θ (ratio of shear stress acting on a particle to its weight) and particle Reynolds number (the ratio of inertial to viscous forces acting on a particle in the flow) has been empirically determined for turbulent flow conditions [Figure 2 in Miller *et al.*, 1977]. However, until recently, there has been little study of particle transport under viscous flow conditions, as would be appropriate for magma flow.

The experimental and theoretical studies of Charru *et al.* [2004] provide a framework for estimating the transport properties of small particles in a uniformly sheared viscous flow. The experiments were conducted in a rotating annular viscous flow, to achieve steady flow over long times and under conditions in which the secondary velocity generated by centrifugal forces was negligible compared to plane Couette flow in the channel. Direct observations showed that small particle motion took the form of a series of saltation “flights,” whose duration τ was found to be independent of shear rate (γ), $\tau \approx 15d_p / v_s$, where d_p is the particle diameter and v_s is the

Stokes settling speed of the particle. The mean particle velocity (\bar{u}) was found to depend linearly on the shear rate, $\bar{u} \approx 0.1\gamma d_p$. The particle flow rate was found to have a quadratic

dependence on shear rate

$$Q_p \approx 0.1\gamma(0.47/d_p)(\theta - 0.12). \quad (25.14)$$

Erosive transport of small particles by fluid flow is a complex process that depends on interaction of the particles and fluid and the particles with each other. Further work is required to understand the flow conditions in magma-waste repository interaction and particle transport under these conditions. However, the scaling arguments presented here form a fundamental framework for estimating transport properties of waste container contents in viscous magma flow. This can be illustrated with simple estimates for magma properties for Yucca Mountain (density of 2750 kg m^{-3} , viscosity of 10 Pa s , 70 vol.% of degassed bubbles 1 mm in diameter), assuming in this example that the magma flow pattern corresponds to flow through a circular cross-section repository drift. The presence of waste containers in the drift will complicate the flow patterns, but the principles illustrated here will hold. For a maximum average velocity of degassed magma in a 5-m-diameter and 1-km-long drift of about 10^{-3} m s^{-1} [using equation (25.12) for the flux] and assuming a standard Poiseuille flow profile for viscous flow in a cylindrical cross-section [Schlichting, 1960], the maximum shear rate 0.1 m above the base of the drift is approximately 7.5 s^{-1} . Using the range of particle sizes and densities for uranium dioxide pellets given previously, the maximum Shields number is about 400 for this viscous flow, corresponding to a maximum particle volumetric flow rate of about $1.6 \times 10^{-13} \text{ m}^3 \text{ s}^{-1}$ in the steady magma circulation setup in the drift [equation (25.13)]. This maximum volumetric flow rate is estimated for the smallest pellets 10 microns in diameter and corresponds to a flow rate of 300 particles per second of this size, assuming the pellets are spherical. This estimate of possible particle transport from disrupted waste containers will be limited by the volume of particles available to the flow.

25.4 Concluding Remarks

25.4.1 Implications of the Models

The models discussed here provide some first order constraints on the interaction of basaltic magma with an open-drift system that is the basis for some potential radioactive waste

repositories. A first order conclusion is that intersected drifts rapidly will be filled by magma. This will be the case irrespective of whether the magma is explosive due to the exsolution and expansion of gases or degassed as a consequence of as yet poorly understood gas segregation processes during ascent. Lejeune *et al.* (this volume) have presented the degassed end member, and we present the explosive case. At typical eruption rates of monogenetic basaltic eruptions (10 to $1,000 \text{ m}^3 \text{ s}^{-1}$), a drift can be filled in a few tens of seconds for the explosive case and a few tens of minutes for the degassed case. Although the magma will quench on contact with the drift walls and containers, estimates of cooling time scales indicate that these effects are small and will not inhibit the filling of the drifts. This view is verified by the observation that basalt flowed along a geothermal borehole for hundreds of meters despite having a volume-to-surface area ratio that is two orders of magnitude smaller than a repository drift.

Characterizing container disruption is complex. In addition to considering the state of magma upon entry into a drift, disruption is also dependent on the design and properties of container materials, particularly in relation to response to impacts and heating. Such considerations go well beyond the scope of this paper, but some inferences can be made. Using the current design concept at Yucca Mountain as an example [CRWMS, 2000], the dynamic pressures even in the fastest explosive flows appear insufficient to cause major damage [Darteville and Valentine, 2005] except close to the dike-drift intersection where the dynamic pressures may be large and the container is rapidly heated and weakened [Woods *et al.*, 2002]. Container failure could occur on a longer time scale due to prolonged heating and pressure effects. Heating weakens the containers, making them more likely to fail, and the interior pressure of the container is expected to increase due to heating of the gases. Simultaneously, the pressure in the surrounding magma after a drift has been filled may increase substantially to lithostatic values or above. For example, if an eruption is occurring, the magma-static pressure at a

300-m-deep repository would be above 8 MPa for a column of degassed magma. Thus, the container might be deformed or broken open, and the contents of the affected containers might be released and transported to the surface.

In the event a drift fills with magma, transport of waste to the surface requires either advective or convective flows. Two scenarios have been investigated that consider magma transport from drifts. Woods *et al.* [2002] described a “dogleg” scenario in which the dike intersects a drift and a secondary fracture develops in a new location along the drift so that once the magma breaches the surface, the magma flows along the drift to connect the inlet dike with the outlet dike. Here, a second scenario is considered where the original supply dike continues to the surface and there is convective exchange between the magma in the drift and the magma flowing up the dike.

In this alternative scenario, Menand and Phillips [2007a; 2007b] infer from their experiments that, independently of moderate changes in the dike magma supply rate, gas segregation processes will occur in the drift and lead to a convective exchange of gas-rich foam and degassed magma flowing out of the drift and back into the dike with bubbly magma from the dike. Using the potential Yucca Mountain repository geometry as an example, flows will likely be in an unstable collapse regime with the gas-rich foam experiencing repeated collapse as it accumulates at the top of the drift. The length and time scales of the gas segregation processes are controlled by the rise of bubbles in the drift. The time required for steady-state gas segregation is estimated to range from hours to hundreds of years depending on the average size of exsolved gas bubbles and on the viscosity of degassed magmas, which depends strongly on the degree of water exsolution, cooling, and crystallization. The associated magma flux is estimated to range from $1 \text{ m}^3 \text{ s}^{-1}$ to $10^{-8} \text{ m}^3 \text{ s}^{-1}$, depending on the magma viscosity and the size of exsolved gas bubbles. The relative proportion of erupted degassed magma depends on the value of the dike magma

supply rate relative to that of the gas segregation flux. If magma is supplied at a higher rate, then gas-rich as well as degassed magmas are expected to be violently erupted; if the supply rate is lower, then mainly degassed magma would be erupted by milder episodic Strombolian explosions generated by the repeated collapse of the foam accumulated at the top of drifts.

A related matter is whether a potential magma flow could transport very dense waste particles. Based on estimates of magma fluxes in the initial stages of basaltic volcanic eruptions, it is unlikely that significant transport of intact waste containers will occur, regardless of whether the flow is unidirectional along the drift [Woods *et al.*, 2002; Darteville and Valentine, 2005] or recirculates within the drift [Menand and Phillips, 2007a, 2007b]. In the event of waste container disruption, estimates suggest that pelletal waste of the size and density used in current design calculations may be transported along the drift in a viscous saltation regime. Two-phase flows of this type have not been widely studied, although recent interest has established the key principles and identified transport regimes [e.g., Charru *et al.*, 2004]. As outlined in this chapter, precise estimates of magma transport dynamics will not become available until the exact configuration of waste containers and drift geometry is known, but the first order estimates presented here suggest that even modest magma shear rates can initiate erosive motion of dense waste pellets along the base of a drift, irrespective of the precise geometric details. For the scenario of volcanic activity interacting with a repository drift, the calculations indicate magma flows are capable of transporting pelletal waste along the drift, with the possibility that this material could be subsequently transported to the surface and may be dispersed in explosive eruptions or effusive flows.

25.4.2 Further Lines of Investigation

The presence of engineered barrier systems and their additional thermal mass will affect the flow of magma within drifts and thus the thermal evolution of the system. Assessing how waste

containers and barrier systems may affect heat transfer into the containers and the cooling rate of magma, as well as gas segregation processes within drifts, is complex and may justify three-dimensional computational modeling.

Confidence in estimates would benefit from improved knowledge of the petrological evolution of magmas during dynamic eruptions as they rise and interact with drifts and their content. This evolution will affect magma viscosity and the size of exsolved gas bubbles, which in turn will exert a strong influence on the fluxes and average velocities associated with gas segregation and convective exchange flow. Constraining the petrological evolution of magmas will improve estimates of the heat transfer and cooling rates during and after gas segregation, and thus the duration of magma exchange flow within repository drifts.

25.5 Suggested Further Reading

White [1979] provides a particularly clear introduction to fluid mechanics with applications to engineering problems including flow in ducts, flow around immersed bodies, and calculations of drag coefficients for various flow configurations. Analytical techniques for the treatment of two-phase flow problems as well as practical applications can be found in Wallis [1969]. Integrating observation, theory, and experimental studies, Sparks *et al.* [1997] provide a technical and complete reference to physical volcanology using historical volcanologic events as case studies.

Acknowledgments: This work benefited from fruitful discussions with Chuck Connor, Brittain Hill, Andrew Hogg, and Gary Matson. This paper was prepared to document work performed by the Center for Nuclear Waste Regulatory Analyses (CNWRA) and its contractors for the U.S. Nuclear Regulatory Commission (NRC) under Contract No. NRC-02-02-012. The activities reported here were performed on behalf of the NRC Office of Nuclear Material Safety

and Safeguards, Division of High-Level Waste Repository Safety. This paper is an independent product of the CNWRA and does not necessarily reflect the view or regulatory position of the NRC.

References

- Bechtel SAIC Company, LLC. 2007. Characterize framework for igneous activity at Yucca Mountain, Nevada. ANL-MGR-GS-000002, Rev. 3. Las Vegas, Nevada: Bechtel SAIC Company, LLC.
- Blackburn, E. A., L. Wilson, and R. S. J. Sparks. 1976. *Journal of the Geological Society of London*, **132**, 429–440.
- Bleise, A., S. R. Danesi and W. Burkhart. 2003. Properties, use and health effects of depleted uranium (DU): a general overview. *J. Environ. Radioactivity*, **64**, 93–112.
- Blundy, J., K. Cashman, and M. Humphreys. 2006. Magma heating by decompression-driven crystallization beneath andesitic volcanoes. *Nature*, **443**, 76–80.
- Bruce, P. M. and H. E. Huppert. 1989. Thermal control of basaltic fissure eruptions. *Nature*, **342**, 665–667.
- Bruce, P. M. and H. E. Huppert. 1990. Solidification and melting along dikes by the laminar flow of basaltic magma. In: Ryan, M. P. (ed.). *Magma Transport and Storage*. John Wiley & Sons, 87–101.
- Carrigan, C. R. 2000. Plumbing Systems. In: Sigurdsson, H., B. F. Houghton, S. R. McNutt, H. Rymer, and J. Stix (eds.). *Encyclopedia of Volcanoes*. Academic Press, 219–235.
- Cashman, K. V. 1992. Groundmass crystallization of Mount St. Helens dacite, 1980–1986—a tool for interpreting shallow magmatic processes. *Contrib. Mineral. Petrol.*, **109**, 431–449.
- Charru, F., H. Mouilleron and O. Eiff. 2004. Erosion and deposition of particles on a bed sheared by a viscous flow. *J. Fluid Mech.*, **519**, 55–80.
- Civilian Radioactive Waste Management System, Management and Operating Contractor. 2000. Total system performance assessment for the site recommendation. TDR-WIS-PA-000001, Rev. 00. ICN01. North Las Vegas, Nevada: DOE, Yucca Mountain Site Characterization Office.

- Dartevelle, S. 2004. Numerical modeling of geophysical granular flows: 1. A comprehensive approach to granular rheologies and geophysical multiphase flows. *Geochem. Geophys. Geosyst.*, **5**, Q08003, doi:10.1029/2003GC000636.
- Dartevelle, S. and G. A. Valentine. 2005. Early-time multiphase interactions between basaltic magma and underground openings at the proposed Yucca Mountain radioactive waste repository. *Geophys. Res. Lett.* **32**, L22311, doi:10.1029/2005GL024172.
- Environmental Protection Agency. 2004. Public Health and environmental radiation protection standards for Yucca Mountain, NV: background information document for 40CFR Part 197.
- Fedotov, S. A. and Ye. K. Markhinin (eds.). 1983. *The Great Tolbachik Fissure Eruption: Geological and geophysical data 1975–1976*. Cambridge University Press.
- Francis, P. and C. Oppenheimer. 2004. *Volcanoes*. Oxford University Press.
- Giordano, D. and D. B. Dingwell. 2003. Viscosity of hydrous Etna basalt: implications for Plinian-style basaltic eruptions. *Bull. Volcanol.*, **65**, 8–14.
- Hess, K.-U. and D. B. Dingwell. 1996. Viscosities of hydrous leucogranitic melts: A non-Arrhenian model. *Am. Mineral.*, **81**, 1,297–1,300.
- Holloway, J. R. and J. G. Blank. 1994. Application of experimental results to C-O-H species in natural melts. In: Carroll, M. R. and J. R. Holloway (eds.). *Volatiles in Magmas*. Reviews in Mineralogy, **30**. Mineralogical Society of America, 187–230.
- Holness, M. B. and M. C. S. Humphreys. 2003. The Traigh Bhàn na Sgùrra Sill, Isle of Mull: Flow localization in a major magma conduit. *J. Petrol.*, **44**, 1,961–1,976.
- Huppert, H. E. and R. S. J. Sparks. 1985. Cooling and contamination of mafic and ultramafic magmas during ascent through continental crust. *Earth Planet. Sci. Lett.*, **74**, 371–386.

- Jaupart, C. 2000. Magma ascent at shallow levels. *In: Sigurdsson, H., B. F. Houghton, S. R. McNutt, H. Rymer, and J. Stix (eds.). Encyclopedia of Volcanoes.* Academic Press, 237–245.
- Jaupart, C. and S. Vergnolle. 1989. The generation and collapse of a foam layer at the roof of a basaltic magma chamber. *J. Fluid Mech.*, **203**, 347–380.
- Kerr, R. C. and J. R. Lister. 1995. Comment on “On the relationship between dike width and magma viscosity” by Yutaka Wada. *J. Geophys. Res.*, **100(B8)**, 15,541.
- Kilburn, C. R. F. 2000. Lava flows and flow fields. *In: Sigurdsson, H., B. F. Houghton, S. R. McNutt, H. Rymer, and J. Stix (eds.). Encyclopedia of Volcanoes.* Academic Press, 291–305.
- Lange, R. A. 1994. Application of experimental results to C-O-H species in natural melts. *In: Carroll, M. R. and J. R. Holloway (eds.). Volatiles in Magmas.* Reviews in Mineralogy, **30**. Mineralogical Society of America, 331–369.
- Larsen, G., K. Grönvold, and S. Thorarinnsson. 1979. Volcanic eruption through a geothermal borehole at Námafjall, Iceland. *Nature*, **278**, 707–710.
- Lejeune, A.-M., A. W. Woods, R. S. J. Sparks, B. E. Hill, and C. B. Connor. The decompression of volatile-poor basaltic magma from a dike into a horizontal subsurface tunnel.
- Lister, J. R. and R. C. Kerr. 1991. Fluid-mechanical models of crack propagation and their application to magma transport in dikes. *Journal of Geophysical Research*, **96**, 10,049–10,077.
- Llewellin, E. W. and M. Manga. 2005. Bubble suspension rheology and implications for conduit flow. *J. Volcanol. Geotherm. Res.*, **143**, 205–217.
- Long, J. C. S. and R. C. Ewing. 2004. Yucca Mountain: Earth-science issues at a geologic repository for high-level nuclear waste. *Annual Review of Earth and Planetary Sciences*. 32:363-401.

- Macdonald, G. A., A. T. Abbott and F. L. Peterson. 1983. *Volcanoes in the Sea: The Geology of Hawaii*. University of Hawaii Press.
- Mason, R. M., A. B. Starostin, O. E. Melnik, and R. S. J. Sparks. 2006. From Vulcanian explosions to sustained explosive eruptions: The role of diffusive mass transfer in conduit flow dynamics. *J. Volcanol. Geotherm. Res.*, **153**, 148–165.
- Massol, H., C. Jaupart, and D. W. Pepper. 2001. Ascent and decompression of viscous vesicular magma in a volcanic conduit. *J. Geophys. Res.*, **106**(B8), 16,223–16,240.
- Melnik, O. and R. S. J. Sparks. 1999. Nonlinear dynamics of lava extrusion. *Nature*, **402**, 37–41.
- Menand, T. and J. C. Phillips. 2007a. Gas segregation in dikes and sills. *J. Volcanol. Geotherm. Res.*, **159**, 393–408.
- Menand, T. and J. C. Phillips. 2007b. A note on gas segregation in dikes and sills at high gas fractions. *J. Volcanol. Geotherm. Res.*, **162**, 185–188.
- Menand T., J. C. Phillips, and R. S. J. Sparks. 2006. Circulation of bubbly magma and gas segregation within tunnels of the potential Yucca Mountain repository. San Antonio, Texas: CNWRA.
- Miller, M. C., N. I. McCave, and P. D. Komar. 1977. Threshold of sediment motion under unidirectional currents. *Sedimentology*, **24**, 507–528.
- Murase, T. and A. R. McBirney. 1973. Properties of some common igneous rocks and their melts at high temperatures. *Geol. Soc. Am. Bull.*, **84**(11), 3,563–3,592.
- National Research Council. 1990. Rethinking high-level radioactive waste disposal. Washington, D.C.: Natl. Acad. Press.
- National Research Council. 2001. Disposition of high-level waste and spent nuclear fuel, the continuing societal and technical challenges. Washington, D.C.: Natl. Acad. Press.

- Nicholis, M. G. and M. J. Rutherford. 2004. Experimental constraints on magma ascent rate for the Crater Flat volcanic zone hawaiite. *Geology*, **32**, 489–492, doi:10.1130/G20324.1.
- NRC. 2005. Integrated issue resolution status report. Vol. 1, Rev. 1. Washington, D.C.: NRC.
- OCRWM. 2000. Miscellaneous Waste-Form FEPs. ANL-WIS-MD-000009 Rev 00 ICN01.
- Petford, N., R. C. Kerr, and J. R. Lister. 1993. Dike transport in granitoid magmas. *Geology*, **21**, 845–848.
- Pinkerton, H. and R. S. J. Sparks. 1978. Field-measurements of the rheology of lava. *Nature*, **276**, 383–385.
- Pollard, D. D. 1987. Elementary fracture mechanics applied to the structural interpretation of dikes. In: Hall, H. C. and W. F. Fahrig (eds.). *Mafic Dike Swarms*. Geologic Association of Canada Special Paper, **34**, 5–24.
- Phillips, J. C. and A. W. Woods. 2001. Bubble plumes generated during recharge of basaltic magma reservoirs. *Earth Planet. Sci. Lett.*, **186**, 297–309.
- Rosseau, J. P., E. M. Kwicklis, and D. C. Giles. 1999. Hydrogeology of the Undersaturated Zone, North Ramp Area of the Exploratory Studies Facility, Yucca Mountain, Nevada. *Water-Resources Investigations Report 98B4050*. U.S. Geological Survey.
- Rubin, A. M. 1995. Propagation of magma-filled cracks. *Annu. Rev. Earth Planet. Sci.*, **23**, 287–336.
- Rubin, A. M. and D. D. Pollard. 1987. Origin of blade-like dikes in volcanic rift zones. *U.S. Geol. Surv. Prof. Pap.*, **1350**, 1,449–1,470.
- Schlichting, H. 1960. *Boundary Layer Theory*. McGraw-Hill.
- Shaw, H. R. 1972. Viscosities of magmatic silicate liquids: An empirical method of prediction. *Am. J. Sci.*, **272**, 870–893.

- Sisson, T. W. and G. D. Layne. 1993. H₂O in basalt and basaltic andesite glass inclusions from four subduction-related volcanoes. *Earth Planet. Sci. Lett.*, **117**, 619–635.
- Slezin, Yu. B. 2003. The mechanism of volcanic eruptions (a steady state approach). *J. Volcanol. Geotherm. Res.*, **122**, 7–50.
- Smith, E.I. and D.L. Keenan. 2005. Yucca Mountain could face greater volcanic threat. *EOS, Transactions, American Geophysical Union*. Vol. 86.
- Sparks, R. S. J. 1978. The dynamics of bubble formation and growth in magmas: a review and analysis. *J. Volcanol. Geotherm. Res.*, **3**, 1–37.
- Sparks, R. S. J. 2003. Dynamics of magma degassing. *In: Oppenheimer, C., D. M. Pyle and J. Barclay (eds.). Volcanic Degassing. Geological Society Special Publications*, **213**, 5–22.
- Sparks, R. S. J., J. Barclay, C. Jaupart, H. M. Mader, and J. C. Phillips. 1994. Physical aspects of magma degassing I. Experimental and theoretical constraints on vesiculation. *In: Carroll, M. R. and J. R. Holloway (eds.). Volatiles in Magmas. Reviews in Mineralogy*, **30**. Mineralogical Society of America, 413–445.
- Sparks, R. S. J., M. I. Bursik, S. N. Carey, J. S. Gilbert, L. S. Glaze, and A. W. Woods. 1997. *Volcanic Plumes*. John Wiley & Sons.
- Spera, F. J. 2000. Physical properties of magma. *In: Sigurdsson, H., B. F. Houghton, S. R. McNutt, H. Rymer and J. Stix (eds.). Encyclopedia of Volcanoes*. Academic Press, 171–190.
- Stephenson, P. J., A. T. Burch-Johnston, D. Stanton, and P. W. Whitehead. 1998. Three long lava flows in north Queensland. *J. Geophys. Res.*, **103**(B11), 27,359–27,370.
- Swanson, D. A., T. L. Wright, and R. T. Helz. 1975. Linear vent systems and estimated rates of magma production and eruption for the Yakima Basalt on the Columbia Plateau. *Am. J. Sci.*, **275**, 877–905.
- Thorarinsson, S. 1969. The Lakagigar eruption of 1783. *Bull. Volcanol.*, **33**, 910–927.

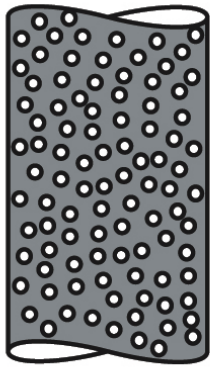
- Turcotte, D. L. and G. Schubert. 1982. *Geodynamics: Applications of Continuum Physics to Geological Problems*. John Wiley & Sons.
- Valentine, G. A., D. J. Krier, F. V. Perry and G. Heiken. 2007. Eruptive and geomorphic processes at the Lathrop Wells scoria cone volcano. *J. Volcanol. Geotherm. Res.*, **161**, 57–80.
- Wada, Y. 1994. On the relationship between dike width and magma viscosity. *J. Geophys. Res.*, **99(B9)**, 17,743–17,755.
- Wada, Y. 1995. Reply. *J. Geophys. Res.*, **100(B8)**, 15,543–15,544.
- Wallace, P. and A. Anderson. 2000. Volatiles in magmas. *In*: Sigurdsson, H., B. F. Houghton, S. R. McNutt, H. Rymer, and J. Stix (eds.). *Encyclopedia of Volcanoes*. Academic Press, 149–170.
- Wallis, G. B. 1969. *One-dimensional Two-phase Flow*. McGraw-Hill.
- White, F. M. 1979. *Fluid Mechanics*. International Student Edition. McGraw-Hill Kogakusha.
- Wilson, L. and J. W. Head. 1981. Ascent and eruption of basaltic magma on the Earth and Moon. *J. Geophys. Res.*, **86**, 2,971–3,001.
- Woods, A. W., S. Sparks, O. Bokhove, A. LeJeune, C. B. Connor, and B. E. Hill. 2002. Modeling magma-drift interaction at the proposed high-level radioactive waste repository at Yucca Mountain, Nevada, USA. *Geophys. Res. Lett.*, **29(13)**, 1,641, doi:10.1029/2002GL014665.

Figure Captions

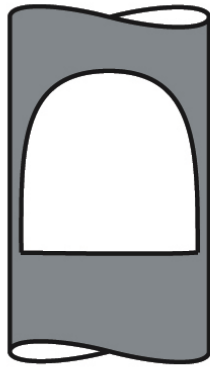
Fig. 25.1. The different flow regimes experienced by two-phase flows, going from bubbly flow to dispersed flow as both gas content and flow explosivity increase.

Fig. 25.2. The coordinate frame used in the one-dimensional simulations of Woods *et al.* [2002].

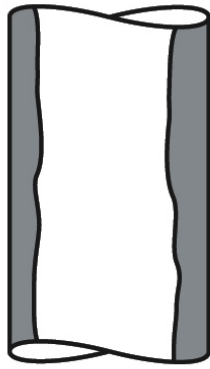
Fig. 25.3. Schematic illustration of magma flow in an interconnecting dike and drift. (a) System geometry. (b) Initial condition with the drift filling with bubbly magma from the dike. (c) Bubble segregation within the drift leads to the formation of a foam layer at the top of the drift and a degassed layer at its floor. (d) Steady-state exchange flows set up by bubble segregation.



bubbly flow



slug flow



annular flow



dispersed flow

Figure 25.1

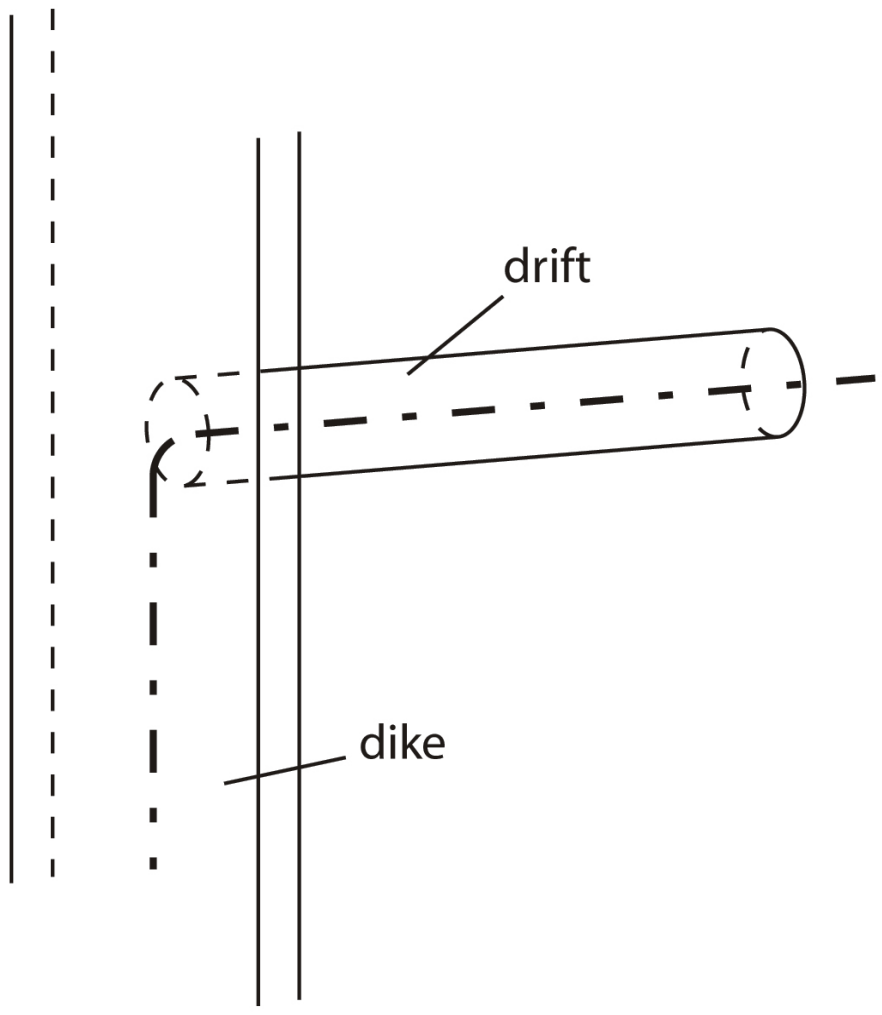


Figure 25.2

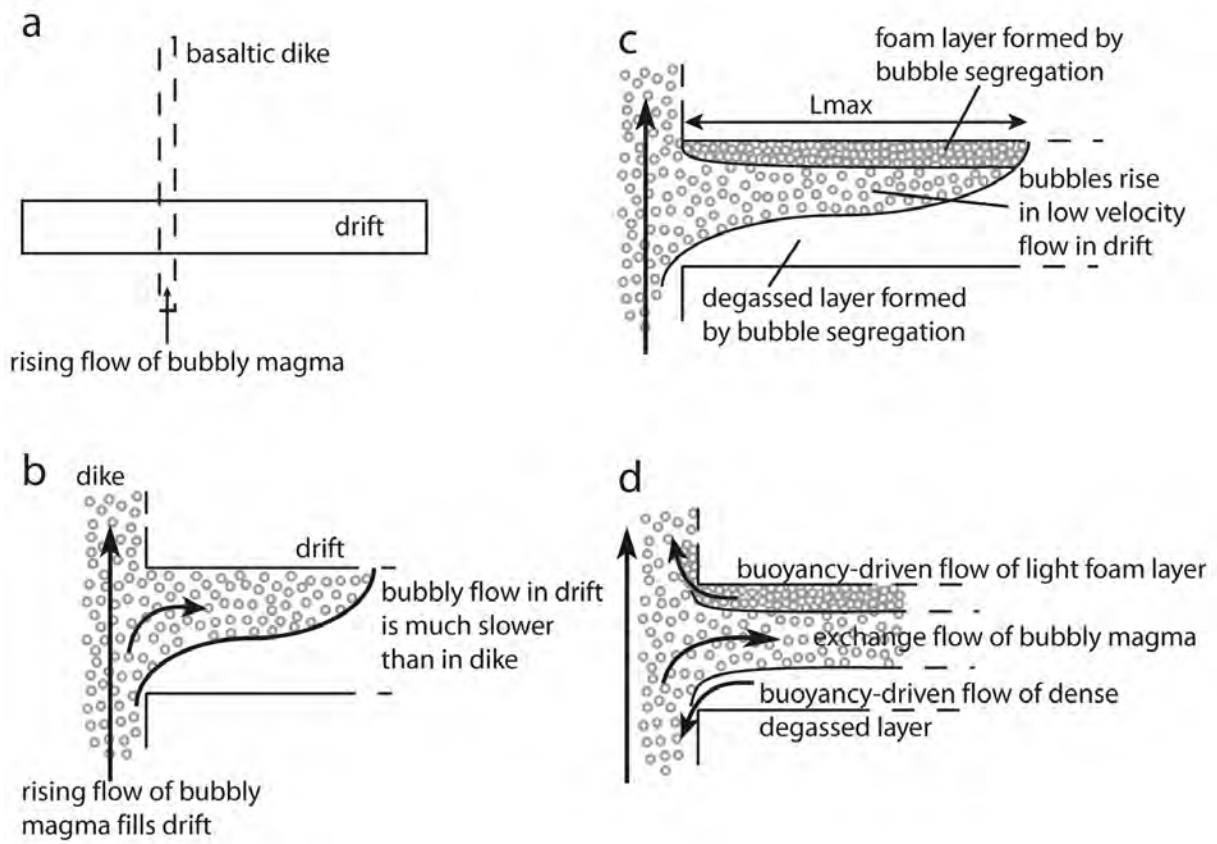


Figure 25.3